

## Characteristics of GaN-based photonic crystal surface emitting lasers

Tien-chang Lu, Shih-Wei Chen, Tsung-Ting Kao, and Tzu-Wei Liu

Citation: *Applied Physics Letters* **93**, 111111 (2008); doi: 10.1063/1.2986527

View online: <http://dx.doi.org/10.1063/1.2986527>

View Table of Contents: <http://scitation.aip.org/content/aip/journal/apl/93/11?ver=pdfcov>

Published by the *AIP Publishing*

---

### Articles you may be interested in

GaN-based surface-emitting laser with two-dimensional photonic crystal acting as distributed-feedback grating and optical cladding

*Appl. Phys. Lett.* **97**, 251112 (2010); 10.1063/1.3528352

Low threshold lasing of GaN-based vertical cavity surface emitting lasers with an asymmetric coupled quantum well active region

*Appl. Phys. Lett.* **93**, 191118 (2008); 10.1063/1.3030876

GaN-based two-dimensional surface-emitting photonic crystal lasers with Al N Ga N distributed Bragg reflector

*Appl. Phys. Lett.* **92**, 011129 (2008); 10.1063/1.2831716

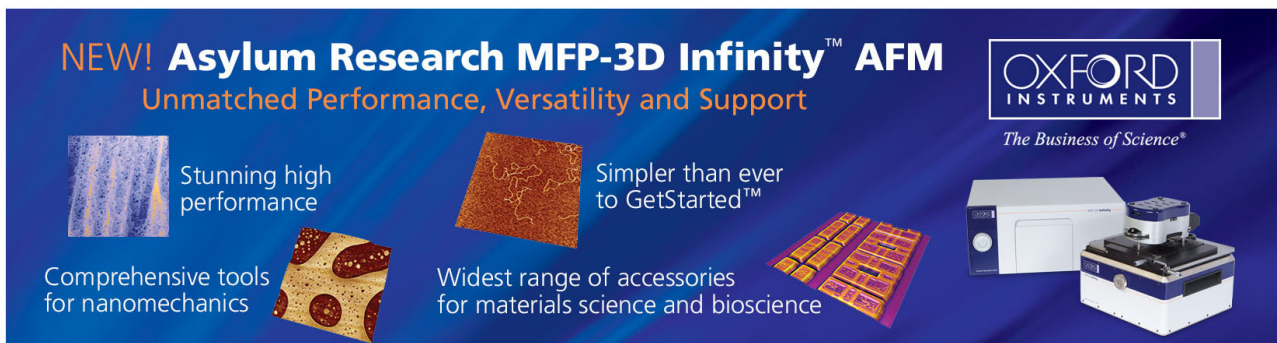
Emission characteristics of optically pumped GaN-based vertical-cavity surface-emitting lasers

*Appl. Phys. Lett.* **89**, 121112 (2006); 10.1063/1.2355476

Low-threshold lasing of InGaN vertical-cavity surface-emitting lasers with dielectric distributed Bragg reflectors

*Appl. Phys. Lett.* **83**, 830 (2003); 10.1063/1.1596728

---



**NEW! Asylum Research MFP-3D Infinity™ AFM**  
Unmatched Performance, Versatility and Support

**OXFORD INSTRUMENTS**  
*The Business of Science®*

Stunning high performance

Simpler than ever to GetStarted™

Comprehensive tools for nanomechanics

Widest range of accessories for materials science and bioscience

# Characteristics of GaN-based photonic crystal surface emitting lasers

Tien-chang Lu,<sup>a)</sup> Shih-Wei Chen, Tsung-Ting Kao, and Tzu-Wei Liu

Department of Photonics and Institute of Electro-Optical Engineering, National Chiao-Tung University, 1001 Ta Hsueh Rd., Hsinchu 30050, Taiwan

(Received 1 April 2008; accepted 28 August 2008; published online 18 September 2008)

Characteristics of GaN-based photonic crystal surface emitting lasers (PCSELs) were investigated and analyzed. The GaN-based PCSEL emits a blue wavelength at 401.8 nm with a linewidth of 1.6 Å and shows a threshold energy density about 2.7 mJ/cm<sup>2</sup> under the optical pumping at room temperature. The lasing wavelength emitted from PCSELs with different lattice constants occurs at the calculated band edges showing different polarization angles due to the light diffracted in specific directions, corresponding exactly to  $\Gamma$ ,  $K$ , and  $M$  directions in the  $K$ -space. Furthermore, the PCSEL also shows a spontaneous emission coupling efficiency  $\beta$  of about  $5 \times 10^{-3}$  and a characteristic temperature of 148 K. © 2008 American Institute of Physics. [DOI: 10.1063/1.2986527]

The multidirectional distributed feedback effect near the band edges in two-dimensional (2D) PC (PC) structures can create a surface emitting laser.<sup>1,2</sup> This kind of PC surface emitting lasers (PCSELs) could be considered as a candidate for perfect single mode emission over a large area, high output power, and surface emission with narrow divergence angle.<sup>3,4</sup> These PCSEL structures are usually composed of a perfect PC lattice and the laser action would happen in those band edge points in the photonic band diagram by satisfying the Bragg condition. The surface emission would occur when the vertical diffraction conditions are satisfied. The PCSELs have been demonstrated by many groups using material systems such as InP, organic, and GaN.<sup>5-8</sup> However, some detailed properties of PCSELs such as emission modes, polarization, characteristic temperature, and spontaneous coupling efficiency have not been reported yet. Recently, we have demonstrated the room temperature lasing action of GaN-based PCSEL structures with bottom AlN/GaN distributed Bragg reflectors.<sup>8</sup> In this letter, we will report the characteristics of GaN-based PCSELs and demonstrate the specific lasing characteristics at the following different band edges:  $\Gamma$ ,  $K$ , and  $M$  points calculated by using the plane-wave expansion method. The lasing modes corresponding to the different points of Brillouin-zone boundary can be confirmed by the polarization directions of the laser emissions.

The GaN-based PCSEL structure was grown by vertical-type metal-organic chemical vapor deposition system. The full epitaxial structure consists of a sapphire substrate, a 35-pairs GaN/AlN bottom DBR, a 560-nm-thick  $n$ -type GaN cladding layer, a ten-pair In<sub>0.2</sub>Ga<sub>0.8</sub>N multiquantum well (MQW), and a 200-nm-thick  $p$ -type GaN cladding layer. The growth details were reported elsewhere.<sup>9</sup> Then, the as-grown sample was deposited with a Si<sub>3</sub>N<sub>4</sub> layer of 200 nm followed by a Polymethylmethacrylate (PMMA) layer of 150 nm. The hexagonal PC patterns were fabricated on the PMMA layer by e-beam lithography and the sample was etched down about 400 nm deep over the MQW layer by dry etching. The hexagonal PC patterns with the lattice constant  $a$  ranging from 175 to 265 nm were defined; and the different circular hole diameter  $r$  over  $a$  ratios were obtained. The whole PC pattern was of a circular shape with a diameter of 50  $\mu\text{m}$ .

Finally, the Si<sub>3</sub>N<sub>4</sub> and PMMA layers were removed by acetone and buffered oxides etch solutions.

The schematic diagram of the overall PCSEL structure is shown in Fig. 1(a). The scanning electron microscopy (SEM) images show the cross section and plane view of the PC structures in Fig. 1(b). The emission spectrum of the GaN-based PC surface emission structure was measured using a microscopy system (WITec, alpha snom). The optical pumping was performed by a Nd:YVO<sub>4</sub> 355 nm pulsed laser with a pulse width of  $\sim 0.5$  ns at a repetition rate of 1 kHz. The pumping laser beam, with a spot size of 50  $\mu\text{m}$ , was normally incident onto the sample surface and covered the whole PC pattern area. A 15 $\times$  objective lens with a numerical aperture of 0.32 was placed normally to the sample to collect the light emission from the top of the PC pattern. The light was then collected through a fiber with a 600  $\mu\text{m}$  core, and coupled into a spectrometer with a charge coupled device. The spectral resolution is about 0.1 nm for spectral output measurement. The GaN-based PCSELs were placed in a cryogenics controlled chamber for obtaining the characteristic temperature. The temperature of the chamber can be controlled from room temperature 300 down to 100 K using the liquid nitrogen.

Figure 2(a) shows the laser intensity as a function of the pumping energy at room temperature condition from the

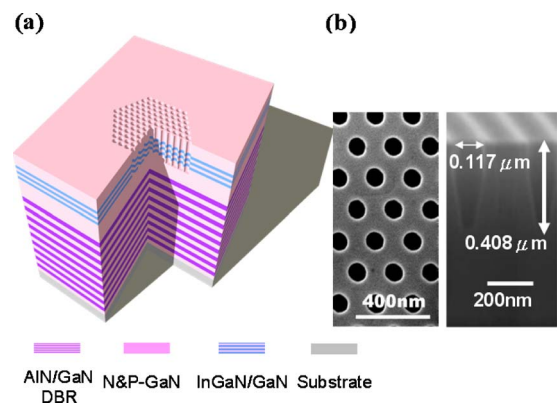


FIG. 1. (Color online) (a) Schematic layer structure of GaN-based PCSELs with a bottom AlN/GaN distributed Bragg reflector. (b) Up: top view and bottom: cross section. SEM images of the PC structures with hexagonal lattices and circle unit cells.

<sup>a)</sup>Electronic mail: timtclu@mail.nctu.edu.tw.

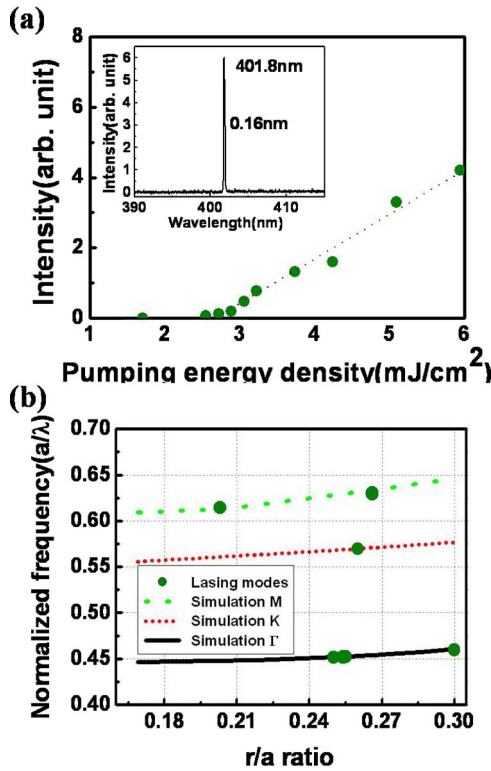


FIG. 2. (Color online) (a) Laser emission intensity as a function of the pumping energy at room temperature condition for the GaN-based PCSEL. The inset shows only one dominant mode appearing in the lasing spectrum. (b) Normalized frequency vs  $r/a$  ratios. The solid (black), dot (red), and dash (green) lines represent the simulation results of  $\Gamma$ ,  $K$ , and  $M$  lasing groups by PWE method. The square points, inserted in the diagram, present the experiment results mapped and compared with the simulation results.

sample with PC lattice constant of 234 nm. The clear evidence of threshold condition occurred at the pumping energy ( $E_{th}$ ) of 165 nJ corresponding to an energy density of 2.7 mJ/cm<sup>2</sup> and the output laser intensity from the sample increased linearly with the pumping energy level beyond the threshold energy. Only one dominated wavelength at 401.8 nm with a linewidth of 1.6 Å was measured, as shown in the inset of Fig. 2(a). Different lasing frequencies were measured from different PC lattice structures. The normalized frequencies as a function of  $r/a$  ratio were plotted as square points in Fig. 2(b). On the other hand, we apply the plane-wave expansion method in two dimensions with an effective index model considering the effects of the partial modal overlap of electromagnetic fields with the PC structures to calculate the band diagram of the hexagonal PC patterns in this structure.<sup>8</sup> The solid (black), dot (red), and dash (green) lines are the calculated band edge frequencies at the  $\Gamma$ ,  $K$ , and  $M$  Brillouin-zone boundaries as a function of  $r/a$  ratio, which were in accordance with the measured results.

The measured polarization curves for different band edge lasers grouped into  $\Gamma$  (red-circle points and solid line),  $K$  (green-triangle points and dot line), and  $M$  (blue-square points and dash line) boundaries calculated by the plane-wave expansion method are shown in Fig. 3(a) and the degree of polarization from the emission defined as  $(I_{max} - I_{min}) / (I_{max} + I_{min})$  was somehow around 50%. The polarization angles from the emissions of devices with different normalized frequencies grouped into  $\Gamma$ ,  $K$  or  $M$  band edge lasers were different. Since the PC lattices provide the optical feed-

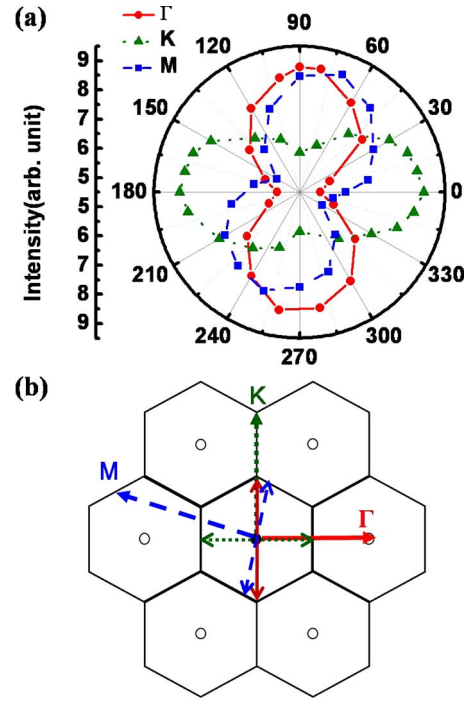


FIG. 3. (Color online) (a) The measured polarization curves for different band edge lasers grouped into  $\Gamma$  (red-circle points and solid line),  $K$  (green-triangle points and dot line), and  $M$  (blue-square points and dash line) boundaries calculated by the plane-wave expansion method. (b) The main polarization directions obtained in (a) and their corresponding diffracted laser beams, which are normal to the polarization directions in a  $K$ -space map corresponding to our hexagonal PC lattice.

back, which is the origin of the band edge laser operation, the direction and the polarization of the laser light will strictly follow the PC lattice vectors. The symmetric feedback directions provided by the 2D lattice vectors could result in a relatively low degree of polarization if the measurement of the polarization is from the top of the device.<sup>10</sup> As a result, it should be rather difficult to distinguish the specific polarization directions in PCSELS when they are categorized as  $\Gamma$ ,  $K$ , or  $M$  band edge lasers. However, the feedback beams could not be equally diffracted by PC lattices probably due to some disorders or imperfections in the structure. This will result in some beams diffracted in specific directions having higher intensity. The ideally symmetric polarization directions will also be broken. The main polarization directions and the main diffracted laser beams, which are normal to the main polarization directions, can be drawn in a  $K$ -space map corresponding to our hexagonal PC lattice, as shown in Fig. 3(b). These main diffracted laser beams, shown as dash lines in Fig. 3(b), point exactly to the  $\Gamma$  (solid-red line),  $K$  (dot-green line), and  $M$  (dash-blue line) boundaries. The distinct polarization directions provide solid evidence that the lasing actions of our PC laser originate from different band edges.

To understand the spontaneous coupling factor  $\beta$  of the GaN-based PCSELS, we further replotted the laser emission intensity versed pumping energy from Fig. 2(a) in logarithmic scale, as shown in Fig. 4(a), and then calculated the difference between the heights of the emission intensities before and after the threshold, corresponding roughly to the value of  $\beta$ . The  $\beta$  value of our PCSEL was estimated to be about  $5 \times 10^{-3}$ . Interestingly, this value is smaller than the GaN-based vertical cavity surface emitting lasers.<sup>11</sup> How-

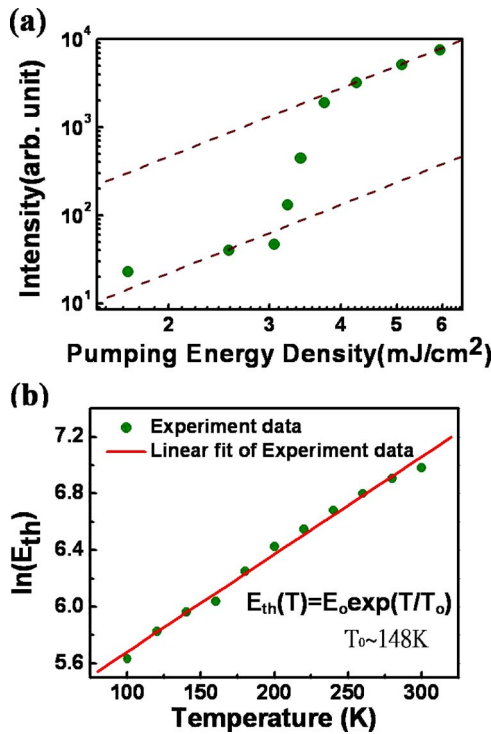


FIG. 4. (Color online) (a) Laser emission intensity vs pumping energy in a logarithmic scale. The  $\beta$  value estimated from the difference between the two dash lines is about  $5 \times 10^{-3}$ . (b) Temperature dependence of the lasing threshold pumping energy ( $E_{th}$ ).

ever, the  $\beta$  factor is still larger than the typical edge emitting lasers (normally about  $10^{-5}$ ) indicating the enhancement in the spontaneous emission into a lasing mode by the high quality factor in GaN-based PCSELS. Figure 4(b) shows the seminatural-logarithm plots of the dependence of the threshold pumping energy [ $\ln(E_{th})$ ] on the operation temperature ( $T_o$ ). The threshold energy gradually increased as the operation rose from 100 to 300 K. The relationship between the threshold energy and the operation temperature could be characterized by the equation:  $E_{th} = E_o \times e^{T/T_o}$ , where  $T_o$  is the characteristic temperature and  $E_o$  is a constant. Therefore, we obtain a characteristic temperature of about 148 K by linear fitting of the experiment data, which is close to the value reported for GaN-based edge emitting lasers.<sup>12</sup>

The performance and characteristics of GaN-based PCSELS were investigated and analyzed. The laser has a threshold pumping energy density of about  $2.7 \text{ mJ/cm}^2$  with PC lattice constant of 234 nm and emits one dominant wavelength of 401.8 nm with a linewidth of about  $1.6 \text{ \AA}$  under the optical pumping at room temperature. The lasing wavelength emitted from GaN-based PCSELS with different lattice constants occurs at the calculated band edges showing different polarization angles indicated different lasing modes corresponding to  $\Gamma$ ,  $K$ , and  $M$  Brillouin-zone boundaries. We further measured the spontaneous coupling factor to be about  $5 \times 10^{-3}$  and the characteristic temperature of 148 K.

The authors would like to gratefully acknowledge S. C. Wang, H. C. Kuo, and P. C. Yu at National Chiao-Tung University and Professor S. H. Fan at Stanford University for their fruitful suggestion. The study was supported by the MOE ATU program, Nano Facility Center and, in part, by the National Science Council in Taiwan under Contract Nos. NSC95-3114-P-009-001-MY2 and NSC96-2120-M009-006.

- <sup>1</sup>M. Meier, A. Mekis, A. Dodabalapur, A. Timko, R. E. Slusher, J. D. Joannopoulos, and O. Nalamasu, *Appl. Phys. Lett.* **74**, 7 (1999).
- <sup>2</sup>M. Imada, S. Node, A. Chutinan, and T. Tokuda, *Appl. Phys. Lett.* **75**, 316 (1999).
- <sup>3</sup>D. Ohnishi, T. Okano, M. Imada, and S. Node, *Opt. Express* **12**, 1562 (2004).
- <sup>4</sup>S. Ogawa, M. Imada, S. Yoshimoto, M. Okano, and S. Noda, *Science* **305**, 227 (2004).
- <sup>5</sup>S. H. Kwon, H. Y. Ryu, G. H. Kim, Y. H. Lee, and S. B. Kim, *Appl. Phys. Lett.* **83**, 3870 (2003).
- <sup>6</sup>M. Notomi, H. Suzuki, and T. Tamamura, *Appl. Phys. Lett.* **78**, 1325 (2001).
- <sup>7</sup>H. Matsubara, S. Yoshimoto, H. Saito, Y. Jianglin, Y. Tanaka, and S. Noda, *Science* **319**, 445 (2008).
- <sup>8</sup>T. C. Lu, S. W. Chen, L. F. Lin, T. T. Kao, C. C. Kao, P. Yu, H. C. Kuo, and S. C. Wang, *Appl. Phys. Lett.* **92**, 011129 (2008).
- <sup>9</sup>G. S. Huang, T. C. Lu, H. H. Yao, H. C. Kuo, S. C. Wang, C. W. Lin, and L. Chang, *Appl. Phys. Lett.* **88**, 061904 (2006).
- <sup>10</sup>H. Y. Ryu, S. H. Kwon, Y. J. Lee, Y. H. Lee, and J. S. Kim, *Appl. Phys. Lett.* **80**, 3476 (2002).
- <sup>11</sup>C. C. Kao, T. C. Lu, H. W. Huang, J. T. Chu, Y. C. Peng, H. H. Yao, J. Y. Tsai, T. T. Kao, and H. C. Kuo, *IEEE Photonics Technol. Lett.* **18**, 877 (2006).
- <sup>12</sup>C. Skierbiszewski, P. Perlin, I. Grzegory, Z. R. Wasilewski, M. Siekacz, A. Feduniewicz, P. Wisniewski, J. Borysiuk, P. Prystawko, G. Kamler, T. Suski, and S. Porowski, *Semicond. Sci. Technol.* **20**, 809 (2005).